Supplementary material to

Onset of Darcy–Bénard convection under throughflow of a shear–thinning fluid

D. Petrolo[1], L. Chiapponi[1], S. Longo[1] , M. Celli[2], A. Barletta[2], V. Di Federico[3]†

[1]Department of Engineering and Architecture - Università degli Studi di Parma - Parco Area delle Scienze 181/A - 43124 Parma - Italy

[2]Department of Industrial Engineering - Alma Mater Studiorum Università di Bologna - Viale Risorgimento 2 - 40136 Bologna - Italy

[3]Department of Civil, Chemical, Environmental, and Materials Engineering - Alma Mater Studiorum Università di Bologna - Viale Risorgimento 2 - 40136 Bologna - Italy

Rheometric measurements and experimental uncertainties

The fluids were prepared by adding Xanthan Gum to softened water in different quantities, adding biocide and sodium chloride as stabiliser, and mixing for several hours in a low-speed stirrer, filtering the mixtures in order to remove lumps. Then rheometric measurements were performed with a parallel plate rheometer (Dynamic Shear Rheometer Anton Paar Physica MCR 101 and Anton Paar MCR702). The mass density was measured with a hydrometer (STV3500/23 Salmoiraghi).

The rheometric parameters have been estimated with a parallel plate rheometer with a gap of 1 mm. Most non–Newtonian fluids show a different behaviour according to the shear–rate range of analysis, hence it is a good practice to identify the range of the expected shear-rate and to focus rheometric experimental analysis in that range (see Longo *et al.* 2013). In the present experiments the instabilities develop in presence of a basic flow with an average shear–rate (in the gap width b) less than 0.4 s^{-1}, hence the rheometric parameters were estimated by collecting data within this range. Figure 1a shows a typical time series of the measured temperatures during one of the text.

Figure 1b shows the shear–rate and viscosity versus shear-stress for a mixture of water and Xanthan Gum (0.20% weight) at $T = 298$ K. At very low shear rate a yield stress can be detected, although it is quite limited for low concentration Xanthan Gum mixtures, see, e.g. Song *et al.* (2006); Benmouffok-Benbelkacem *et al.* (2010).

The overall uncertainty associated with the rheometric parameters is $\Delta\mu_0^*/\mu_0^* \leqslant 3\%$ and $\Delta n/n \leqslant 2\%$. The slope of the consistency index ξ was estimated with the methodology detailed in Celli *et al.* (2017), resulting in $\xi = 0.09 \pm 0.01$ K^{-1}. A second validation of the model for describing $\mu^*(T)$ was performed with the use of rheometric measurements. Figure 2ab shows the temperature effects on shear-stress–shear-rate relationship and on the apparent viscosity, for the power–law fluid used for Expt 7. The parameter ξ has been estimated by fitting the relation (Nowak *et al.* 1982; Celli *et al.* 2017),

$$\mu^*(T) = \frac{\mu_0^*}{[1 + \xi(T - T_0)]^n}, \tag{S.1}$$

† Email address for correspondence: vittorio.difederico@unibo.it

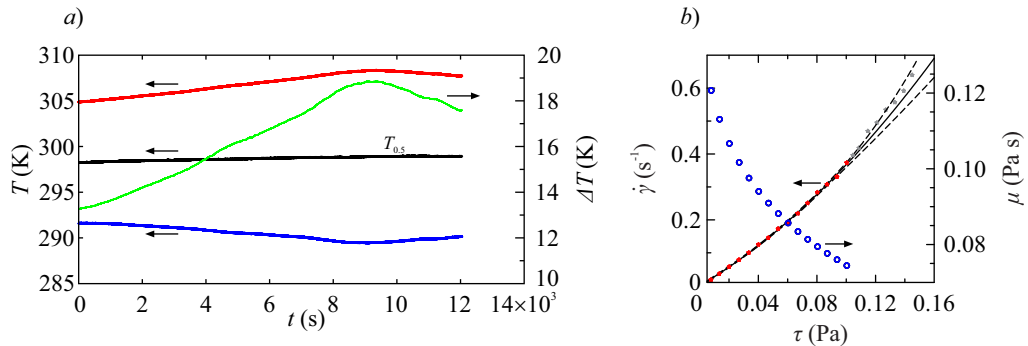2   *D. Petrolo, L. Chiapponi, S. Longo, M. Celli, A. Barletta, V. Di Federico*

Figure S1: *a*) Temperature variations during one experiment (Expt 4). The upper and lower curves refer to the cold and hot frame, respectively, with the temperature at mid-height, $T_{0.5}$, represented by the black curve. The green curve represents the temperature difference between the two frames. *b*) Viscometric behaviour of the mixture of Xanthan Gum (0.20 % weight) in water at $T = 298$ K; the shear-rate (stars) and the viscosity (circles) are plotted versus the shear-stress. The interpolating (continuous) curve is based only on data with $\dot{\gamma} < 0.4$ s^{-1}, the dashed curves are the limits of confidence at the 95% level. The grey symbols refer to experimental values above the maximum threshold chosen for detecting the rheometric parameters. A linear plot was chosen instead of the classic bilogarithmic plot, as it is more useful for showing the full range of the limited shear-rate/shear-stress variation.
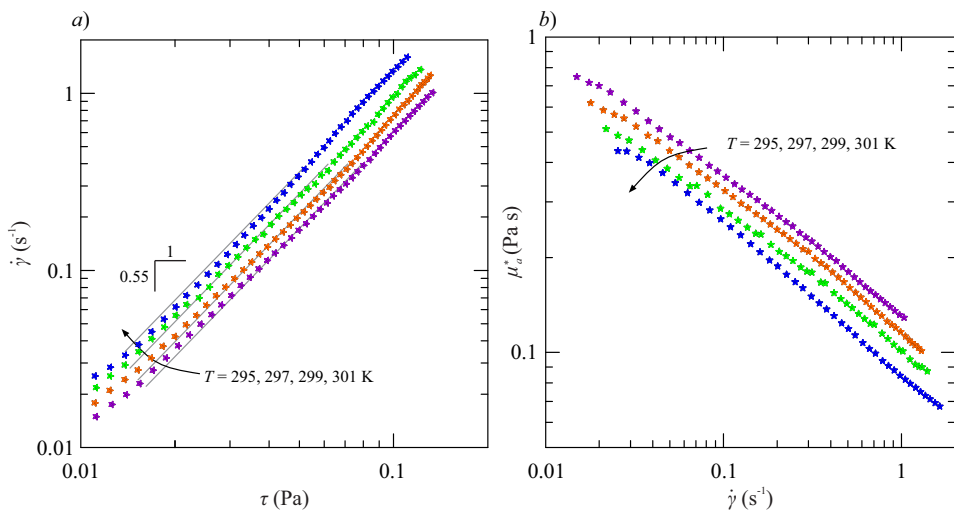

Figure S2: Rheometric data for a power–law fluid used for Expt 7. *a*) Measured shear-stress versus shear-rate, and *b*) apparent viscosity μ_a^* versus shear-rate for different temperatures. Symbols are measurements, lines are the interpolating function (S.1) with a fixed value of the fluid behaviour index $n = 0.55$.

where μ_0^* is the consistency index at the nominal temperature T_0. Other models are available, e.g., (Darbouli *et al.* 2016):

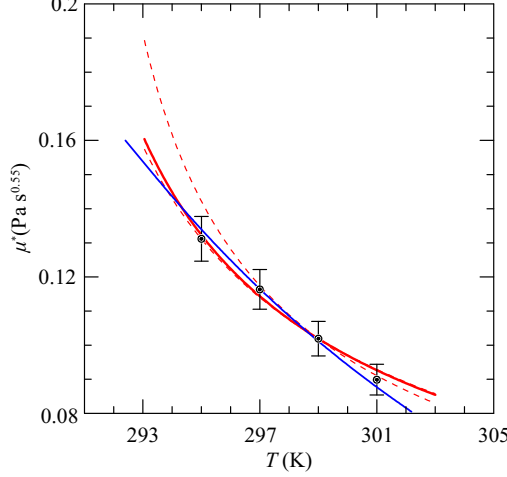$$\mu^*(T) = \frac{\mu_0^*}{\exp[k(T - T_0)]}. \tag{S.2}$$

Figure S3: Variation of the consistency index with temperature. The continuous red line is the interpolation of eq.(S.1), the hyperbolic model, the dashed lines are the limits of confidence at 95%; the continuous blue line is the interpolation according to eq.(S.4), the negative exponential model. Symbols are experimental data results with error bars equal to 2 standard deviations.

Figure 3 shows the interpolation for both models, with an almost equivalent agreement. The new estimation of the parameter is $\xi = 0.10 \pm 12\%$, which well compares with the value $\xi = 0.09 \pm 0.01$ obtained with the methodology detailed in Celli *et al.* (2017); the exponential model gives $k = 0.07 \pm 8\%$. For comparison, expanding in series the hyperbolic model yields

$$\mu^*(T) = \frac{\mu_0^*}{[1 + \xi(T - T_0)]^n} \equiv \frac{\mu_0^*}{1 + n\xi(T - T_0) + O(\xi^2(T - T_0)^2)}, \qquad (S.3)$$

while expanding the exponential model yields

$$\mu^*(T) = \frac{\mu_0^*}{\exp[k(T - T_0)]} \equiv \frac{\mu_0^*}{1 + k(T - T_0) + O(k^2(T - T_0)^2)}, \qquad (S.4)$$

with $k = n\xi$.

The uncertainty on the cell gap and on the windows thickness is 10^{-2} cm, the uncertainty on the cell height is 10^{-1} cm. The cell permeability has been computed as $K = (b/2)^{n+1}[n/(2n+1)]^n$ and $\Delta K / K \leqslant 7.5\%$. The thermal diffusivity of the cell has been evaluated as a weighted average $\chi = \chi_f b/Y + \chi_w(1 - b/Y)$, where $\chi_f = 1.43 \times 10^{-7}$ m^{2}s^{-1} is the thermal diffusivity of the fluid and $\chi_w = 1.22 \times 10^{-7}$ m^{2}s^{-1} is the thermal diffusivity of the plastic walls, both known with absolute uncertainty of 10^{-9} m^{2}s^{-1}. These data yield $\Delta \chi / \chi \leqslant 4\%$.

The mass density has $\Delta \rho / \rho \leqslant 0.1\%$ and the thermal expansion coefficient, assumed on the basis of data from literature equal to $\beta = 2.02 \times 10^{-4}$ K^{-1}, has an uncertainty $\Delta \beta / \beta \leqslant 1\%$.

The flow velocity has been estimated (i) by measuring the flow discharge of the injection pump, and (ii) adopting Particle Image Velocimetry (see Celli *et al.* 2017, for details), with an overall uncertainty in the basic flow velocity equal to $\Delta \overline{u_b}/\overline{u_b} \leqslant 1\%$. The absolute uncertainty in temperature difference is equal to 0.12 K and, on the basis of

the uncertainty of the variables, the overall uncertainty on Péclet and Rayleigh numbers is $\Delta Pe/Pe \leqslant 7.5\%$ and $\Delta Ra_c/Ra_c \leqslant 40\%$, respectively.

The wavelength of the instabilities has been estimated by (i) extracting the frames showing the tracer line injected at mid-section $z/H = 0.5$ at the early stages of distortion, (ii) approximating the curve by eye with a pointer and recording the pixels position, (iii) applying a further transformation from pixels into physical coordinates. Then a sinusoid has been fitted to the extracted data, estimating the wavelength with an absolute uncertainty $\leqslant 0.2$ cm. The procedure has been repeated for several frames in order to obtain consistent estimators of the average wavelength and of the variance.

Acknowledgements

REFERENCES

BENMOUFFOK-BENBELKACEM, G., CATON, F., BARAVIAN, C. & SKALI-LAMI, S. 2010 Nonlinear viscoelasticity and temporal behavior of typical yield stress fluids: Carbopol, Xanthan and Ketchup. *Rheologica Acta* **49** (3), 305–314.

CELLI, M., BARLETTA, A., LONGO, S., CHIAPPONI, L., CIRIELLO, V., DI FEDERICO, V. & VALIANI, A. 2017 Thermal instability of a power-law fluid flowing in a horizontal porous layer with an open boundary: a two-dimensional analysis. *Transport in Porous Media* **118** (3), 449–471.

DARBOULI, M., MÉTIVIER, C., LECLERC, S., NOUAR, C., BOUTEERA, M. & STEMMELEN, D. 2016 Natural convection in shear-thinning fluids: Experimental investigations by MRI. *International Journal of Heat and Mass Transfer* **95**, 742–754.

LONGO, S., DI FEDERICO, V., CHIAPPONI, L. & ARCHETTI, R. 2013 Experimental verification of power-law non-Newtonian axisymmetric porous gravity currents. *Journal of Fluid Mechanics* **731**, R2.

NOWAK, Z., GRYGLASZEWSKI, P. & STACHARSKA-TARGOSZ, J. 1982 Laminar heat transfer to power law fluids in flat gaps with various thermal wall conditions. *Acta Mechanica* **44**, 223–236.

SONG, K.-W., KIM, Y.-S. & CHANG, G.-S. 2006 Rheology of concentrated Xanthan Gum solutions: Steady shear flow behavior. *Fibers and Polymers* **7** (2), 129–138.